Inorg. Chem. **2007**, *46*, 1018–1026

Complexation of Pu(IV) with the Natural Siderophore Desferrioxamine B and the Redox Properties of Pu(IV)(siderophore) Complexes

Hakim Boukhalfa, Sean D. Reilly, and Mary P. Neu*

Inorganic, Isotope and Nuclear Chemistry (C-IIC), Los Alamos National Laboratory, Los Alamos, New Mexico 87545

Received August 15, 2006

The bioavailability and mobility of Pu species can be profoundly affected by siderophores and other oxygen-rich organic ligands. Pu(IV)(siderophore) complexes are generally soluble and may constitute with other soluble organo-Pu(IV) complexes the main fraction of soluble Pu(IV) in the environment. In order to understand the impact of siderophores on the behavior of Pu species, it is important to characterize the formation and redox behavior of Pu(siderophore) complexes. In this work, desferrioxamine B (DFO-B) was investigated for its capacity to bind Pu(IV) as a model siderophore and the properties of the complexes formed were characterized by optical spectroscopy measurements. In a 1:1 Pu(IV)/DFO-B ratio, the complexes Pu(IV)(H_2DFO-B)$^{4+}$, Pu(IV)(H_1DFO-B)$^{3+}$, Pu(IV)(DFO-B)$^{2+}$, and Pu(IV)(DFO-B)(OH)$^{+}$ form with corresponding thermodynamic stability constants log $\beta_{1,1,2} = 35.48$, log $\beta_{1,1,1} = 34.87$, log $\beta_{1,1,0} = 33.98$, and log $\beta_{1,1,-1} = 27.33$, respectively. In the presence of excess DFO-B, the complex Pu(IV)H_2(DFO-B)$_2^{2+}$ forms with the formation constant log $\beta_{2,1,2} = 62.30$. The redox potential of the complex Pu(IV)H_2(DFO-B)$_2^{2+}$ was determined by cyclic voltammetry to be $E_{1/2} = -0.509$ V, and the redox potential of the complex Pu(IV)(DFO-B)$^{2+}$ was estimated to be $E_{1/2} = -0.269$ V. The redox properties of Pu(IV)(DFO-B)$^{2+}$ complexes indicate that Pu(III)(siderophore) complexes are more than 20 orders of magnitude less stable than their Pu(IV) analogues. This indicates that under reducing conditions, stable Pu(siderophore) complexes are unlikely to persist.

Introduction

Nuclear materials production and processing for power plants and the weapons industries have resulted in the release of actinides in the environment. Soils and groundwater sediments contaminated with actinides are present at many facilities operated by the Department of Energy.[1] The behavior of radionuclide contaminants in these systems depends on the composition and the biogeochemistry of the contaminated site. Bacteria can significantly impact the geochemical conditions at multiple scales and also interact with actinides via direct and indirect mechanisms. Understanding the fundamental aspects of microorganism interactions with plutonium is important for the long-term monitoring, predictive modeling, and possible bioremediation of the contaminated sites.

Bacteria can affect plutonium speciation through processes such as reduction,[2−4] bioadsorption,[5,6] and bioaccumulation.[7] However, the form of plutonium defines the extent of these interactions and how they affect its environmental behavior. Organic chelators, which have high binding affinities toward plutonium species, may affect plutonium−bacterial interactions by increasing plutonium bioavailability, solubility, and redox behavior.[8] A number of natural and synthetic chelators present in environmental systems can interact with plutonium and affect its speciation. Among the naturally occurring

* To whom correspondence should be addressed. E-mail: mneu@lanl.gov. Fax: 505-667-9905. Phone: 505-667-7717.

(1) Riley, R. G.; Zachara, J. M. U.S. Department of Energy, Office of Energy Research, Subsurface Science Program, Report DOE/ER-0547-T, 1992.
(2) Lovley, D. R.; Phillips, E. J. P.; Gorby, Y. A.; Landa, E. R. *Nature* **1991**, *350*, 413−416.
(3) Lloyd, J. R.; Yong, P.; Macaskie, L. E. *Environ. Sci. Technol.* **2000**, *34*, 1297−1301.
(4) Neu, M. P.; Icopini, G. A.; Boukhalfa, H. *Radiochim. Acta* **2005**, *93*, 705−714.
(5) Gillow, J. B.; Dunn, M.; Francis, A. J.; Lucero, D. A.; Papenguth, H. W. *Radiochim. Acta* **2000**, *88*, 769−774.
(6) Haas, J. R.; Dichristina, T. J.; Wade, R. *Chem. Geol.* **2001**, *180*, 33−54.
(7) John, S. G.; Ruggiero, C. E.; Hersman, L. E.; Tung, C. S.; Neu, M. P. *Environ. Sci. Technol.* **2001**, *35*, 2942−2948.
(8) Icopini, G. A.; Boukhalfa, H.; Neu, M. P. *Env. Sci. Technol*. **2007**, in press.

10.1021/ic061544q CCC: $37.00 © 2007 American Chemical Society
Published on Web 01/11/2007

plutonium oxidation states, the tetravalent state is of particular interest because of its broad stability range and also because of its reactivity, which is in many aspects similar to that of ferric iron. Both metal ions have strong Lewis acidities and hydrolyze at relatively low pH. The resulting hydroxides are highly insoluble, and the concentrations of their free metal ions in solution at neutral pH are very low, as indicated by their respective solubility products, log K_s $Fe(OH)_4 = -38.6$[9] and log $K°_s$ (PuO_2, am, hydr) $= -58$.[10] Natural siderophores, which are secreted by microorganisms to bind iron and mediate its transport to the cell, constitute a major class of naturally occurring chelators that also bind plutonium. Siderophores, which are common in soil and marine environments (0.1−0.01 μM in soils)[11] usually include hydroxamate, catecholate, and carboxylic acid functional groups. These binding groups, rich in hard oxygen donors, have large binding affinities for hard metal ions like Fe(III)[12] and Pu(IV).[13] Most siderophores are hexadentate and fully coordinate Fe(III) to form 1:1 Fe(III)/siderophore complexes. Siderophore complexes of Pu(IV) have stoichiometries significantly different from that of Fe(III)(siderophore) complexes because Pu(IV) has higher coordination numbers (typically from 8 to 12). As a result, Pu(IV) can form 1:1 Pu(IV)/siderophore complexes (Pu(IV)(siderophore)-$(H_2O)_n$), hydrolysis products (Pu(IV)(siderophore)$(OH)_x(H_2O)_{n-x}$), and also 1:2 Pu(IV)/siderophore complexes (Pu(IV)-$(siderophore)_2(H_2O)_n$). Siderophores have been shown to solubilize Pu(IV) hydroxides, mediate Pu(IV) uptake by microorganisms,[7] and mobilize plutonium and uranium bound to mineral surfaces.[14,15]

There are few studies that investigated the formation and the redox properties of Pu(IV)(chelate) complexes[16,17] and Pu(IV) complexes with biogenic organic ligands that might influence Pu behavior in the environment remain unexplored. The single-crystal X-ray diffraction structure of the Pu(IV)-(desferrioxamine E) reported earlier shows that Pu(IV) can form a stable monometallic complex with the tris hydroxamate siderophore desferrioxamine E.[13] The first coordination shell of Pu(IV) is composed of six oxygens from the siderophore and three oxygens from water. This structure shows that a single siderophore molecule cannot fully coordinate Pu(IV) and that Pu(IV) can accommodate more donor groups from another siderophore molecule.

The present paper presents the thermodynamic and electrochemical characterization of Pu(IV)(DFO-B) complexes. The formation of the complex $Pu(IV)(DFO\text{-}B)^{2+}$, its protonation, and hydrolysis have been determined by spectrophotometric measurements. The formation of the complex $Pu(IV)H_2(DFO\text{-}B)_2{}^{2+}$ has also been studied by spectrophotometric measurements, and its thermodynamic stability constant determined. The redox potentials of Pu(IV)(DFO-$B)^{2+}$, $Pu(IV)H_n(DFO\text{-}B)_2{}^{n+}$, and their analogue complexes formed with other natural siderophores such as desferrioxamine E, pyoverdin, and rhodotorulic acid have been examined. The redox behaviors of Pu(IV) complexes are compared with their Fe(III) analogues and discussed in terms of Pu interactions with microorganisms and the stability of its siderophore complexes in the environment.

Experimental Section

Materials. All solutions were prepared with deionized water. Desferrioxamine B ($H_3DFO\text{-}B^+$) (in the form of methanesulfonate salt) and rhodotorulic acid (RA) were purchased from Aldrich and used without further purification. Desferrioxamine E was obtained from Prof. G. Winkelmann, Microbiology/Biotechnology, University of Tuebingen, Tuebingen, Germany. Pyoverdin was purified from iron-starved *Pseudomonas putida* cultures and its purity checked by mass spectrometry and NMR.[18] Plutonium(IV) stock solution was prepared from Pu metal by acid dissolution. Plutonium metal was dissolved in chilled 6 M HCl to give a Pu(III) solution (isotopic composition: 94% ^{239}Pu; 6% ^{240}Pu; trace ^{238}Pu, ^{241}Pu, and ^{242}Pu). The Pu(III) solution was mixed with an equal volume of 16 M HNO_3 to give a Pu(IV) solution. The Pu(IV) solution was purified using anion-exchange chromatography.[19] The concentration of Pu(IV) stock solutions was determined spectrophotometrically using the absorbance band at 470 nm and a molar absorptivity coefficient of 56 M^{-1} cm^{-1}. The NaOH titrant used for potentiometric titration was standardized against potassium hydrogen phthalate, and the amount of dissolved carbonate remained less than 1%, as determined by Gran's method.[20] A stock solution of 1.0 M sodium nitrate prepared by dissolving sodium nitrate salt in water was used to adjust the ionic strength. All other reagents were purchased from common chemical suppliers and used without any further purification.

Spectrophotometric Measurements. The UV−visible spectra were collected using a Varian Cary 6000i spectrophotometer with a 0.20 nm bandwidth. All the measurements were made using a 1.0 cm quartz cuvette at 25 °C. The ionic strength was fixed at $I =$ 0.10 M using sodium nitrate. The concentration of DFO-B was determined spectrophotometrically after complexation with Fe(III).[21] All $p[H^+]$ measurements were conducted with a Fisher Scientific AR 15 pH meter connected to an Orion ROSS combination pH electrode filled with 3.0 M aqueous sodium nitrate. The pH electrode was calibrated using a six-point calibration with standard solutions of hydrochloric acid (HCl) and sodium hydroxide (NaOH) in 0.10 M sodium nitrate to directly measure $-\log [H^+]$. The acid

(9) Martell, A. E.; Smith, R. M. *Critical Stability Constants*; Plenum Press: New York, 1989; Vol. 4: Inorganic Complexes.
(10) Guillaumont, R.; Fanghänel, T.; Fuger, J.; Grenthe, I.; Neck, V.; Palmer, D. A.; Rand, M. H. *Update on the Chemical Thermodynamics of Uranium, Neptunium, Plutonium, Americium, and Technetium*; Elsevier: Amsterdam, 2003; Vol. 5.
(11) Powell, P. E.; Cline, G. R.; Reid, C. P. P.; Szaniszlo, P. J. *Nature* **1980**, *287*, 833−834.
(12) Crumbliss, A. L. In *Handbook of Microbial Iron Chelates*; Winkelmann, G., Ed.; CRC Press: Boca Raton, FL, 1991; pp 177−233.
(13) Neu, M. P.; Matonic, J. H.; Ruggiero, C. E.; Scott, B. L. *Angew. Chem., Int. Ed.* **2000**, *39*, 1442−1444.
(14) Hakem, N. L.; Allen, P. G.; Sylwester, E. R. *J. Radioanal. Nucl. Chem.* **2001**, *250*, 47−53.
(15) Burns, C. J.; Neu, M. P.; Boukhalfa, H.; Gutowski, K. E.; Bridges, N. J.; Rogers, R. D. In *Comprehensive Coordination Chemistry II*; McCleverty, J. A., Meyer, T. J., Eds; Elsevier Ltd.: Oxford, U.K., 2004; Vol. 3, pp 189−345.
(16) Bouby, M.; Billard, I.; MacCordick, J.; Rossini, I. *Radiochim. Acta* **1998**, *80*, 95−100.
(17) Boukhalfa, H.; Reilly, S. D.; Smith, W. H.; Neu, M. P. *Inorg. Chem.* **2004**, *43*, 5816−5823.
(18) Boukhalfa, H.; Reilly, S. D.; Michalczyk, R.; Iyer, S.; Neu, M. P. *Inorg. Chem.* **2006**, *45*, 5607−5616.
(19) Reilly, S. D.; Neu, M. P. *Inorg. Chem.* **2006**, *45*, 1839−1846.
(20) Martell, A. E.; Motekaitis, R. J. *Determination and Use of Stability Constants*, 2nd ed.; VCH publishers: New York, 1992.
(21) Monzyk, B.; Crumbliss, A. L. *J. Am. Chem. Soc.* **1982**, *104*, 4921−4929.

concentrations of solutions whose acidity was below $p[H^+] = 1.5$ were calculated from the amounts of the hydrochloric acid stock solution added. The electronic absorption spectra of acidic solutions containing DFO-B were recorded immediately after the addition of DFO-B by assuming that the equilibrium involved is rapidly established. This was necessary to minimize the effects of DFO-B hydrolysis, which occurs in strong acid. At higher pH (pH > 2.5), the electronic absorption spectra of Pu(IV)(DFO-B) solutions were measured at each $p[H^+]$ when equilibrium was reached. The $p[H^+]$ was increased by incremental additions of known volumes of standardized sodium hydroxide solutions (1.0 or 0.10 M) to the solutions maintained under constant stirring. All the titrations were performed from low to high pH. The reversibility of the reactions studied was established by comparing the spectra of solutions at the same pH before and after the titration. The amounts of acid or base added were too small to affect the overall volume, and no dilution factor was applied to the data. Two titrations were performed to determine the stoichiometry of the complexes formed. The first titration was performed by recording the electronic absorption spectra of solutions with equimolar concentrations of Pu(IV) and DFO-B from $p[H^+] = 0.25$ to 8.55. The concentrations of the species in solution were [Pu(IV)] = [DFO-B] = 0.59 mM. The second titration was performed by recording the electronic absorption spectra of solutions with 2 equiv of DFO-B and 1 equiv of Pu(IV). The titration of the complex $Pu(IV)(DFO\text{-}B)_2$ ([Pu(IV)] = 0.59 mM and [DFO-B] = 1.20 mM) was performed in the $p[H^+]$ range from $p[H^+] = 0.25$ to 6.47. The spectrophotometric data were analyzed using the program LETAGROP-SPEFO.[22]

Potentiometric Measurements. All potentiometric measurements were conducted on stirred solutions in a water-jacketed vessel at 25.0 ± 0.1 °C under ultrapure argon atmosphere. The ionic strength was fixed at 0.10 M using sodium nitrate. Titrants were dispensed using a Brinkmann Metrohm 665 Dosimat. Potentiometric measurements were made using an Orion Research EA940 pH meter and an Orion ROSS combination pH electrode filled with 3.0 M aqueous sodium nitrate. The pH electrode was calibrated by an acid−base titration before each titration to directly measure $-\log [H^+]$. The titration of free DFO-B (0.021 mmol, pH 2.16−11.87) was performed by incremental addition (0.05 mL) of standardized sodium hydroxide (NaOH, 0.1014 M) to the ligand solution maintained under argon and constant stirring. The titrations of Pu(IV)(DFO-B) complex (0.0198 mmol of DFO-B and 0.0198 mmol of Pu(IV) from $p[H^+]$ 1.43 to 11.86) and $Pu(IV)(DFO\text{-}B)_2$ (0.0198 mmol of Pu(IV) and 0.0396 mmol of DFO-B from $p[H^+]$ 1.18 to 11.86) were performed similarly. Experimental data were modeled numerically using the program SUPERQUAD.[23] A pK_w of 13.78 (0.10 M ionic strength $NaNO_3$, 25 °C) was used in all calculations.

Electrochemistry. All solutions were prepared with argon saturated deionized water and the ionic strength was fixed at 0.10 M using sodium nitrate ($NaNO_3$). Electrochemical measurements were performed using a bi-potentiostat-galvanostat, model INCCHI700B from Chinstruments, Inc. All measurements were made in a small-volume cell (3 mL) using a conventional three-electrode cell: reference electrode Ag/AgCl BAS model RE-5 (MF-2079) filled with a 3.0 M NaCl solution saturated with AgCl, platinum wire as an auxiliary electrode, and a glassy carbon working electrode BAS MF-2012 (3.0 mm disk diameter). The working electrode was prepared by light polishing with fine 0.05 μm alumina. Better reproducibility was obtained by repolishing the surface of the electrode prior to each measurement. The reference electrode was tested for viability by reading the potential difference with the same type of electrode submersed in 3.0 M NaCl solution. The actual differences measured were typically within acceptable potential differences (<20 mV). Cyclic voltammograms were recorded between −1.0 and +1.0 V at a scan rate of 100 mV/s. The Pu(IV)(siderophore) complexes were prepared by adding 1.2 equiv of a siderophore to an acidic solution containing 1 equiv of Pu(IV). The pH was immediately raised above 2 to avoid siderophore hydrolysis. The concentrations of the Pu(IV)(siderophore) complexes were 2.0 mM, and the pH was adjusted to the desired value by addition of sodium hydroxide. The 1:2 Pu(IV)/siderophore complexes were prepared similarly by adding excess siderophore (50 equiv) to 1 equiv of Pu(IV). The Fe(III)(siderophore) complexes were prepared by adding 1.2 equiv of siderophore to an acidic solution of Fe(III). The pH of the metal complex solutions was adjusted by addition of sodium hydroxide and measured using a Fisher Scientific AR 15 pH meter equipped with an Orion ROSS semi-micro combination electrode. The electrode was filled with a 3.0 M $NaNO_3$ solution and calibrated using a three-point calibration method using pH 4.0, 7.0, and 10.0 buffers. All redox potentials given in the text were converted to give reading versus NHE.

Results and Discussion

Desferrioxamine B (DFO-B) Deprotonation Constants. The potentiometric titration of free DFO-B in aqueous solution (Figure S1 in Supporting Information) shows the titration of several protons above pH 7. The values of the deprotonation constants Ka_n (eq 1) determined under our experimental conditions are shown in Table 1 along with selected protonation constants from the literature included for comparison.

$$Ka_n = \frac{[H_{3-n}DFO\text{-}B^{1-n}][H^+]}{[H_{4-n}DFO\text{-}B^{2-n}]} \quad (1)$$

The three deprotonation constants determined are easily assigned to the deprotonation of the three hydroxamate binding groups within DFO-B. The values determined compare well with the values from the literature.[24,25] The deprotonation constant of the primary amine group of DFO-B occurs at the limit of the pH accessible to potentiometric measurements and was not determined. The primary amine remains protonated in the $p[H^+]$ domains examined here ($p[H^+] < 11$). By taking into account the deprotonation sites of DFO-B, the fully protonated ligand is denoted $H_3DFO\text{-}B^+$.

Overall Complex Stability Determination. The accurate determination of the thermodynamic stability constants for Pu(IV) binding by natural siderophores is challenging because most siderophores have a low stability in strong acid solutions. The free concentration of Pu(IV) in the pH domains where siderophores are sufficiently stable is too low to allow the determination of the equilibrium constant. DFO-B, like most natural siderophores, undergoes rapid hydrolysis

(22) Sillen, L. G.; Warnquist, B. *Ark. Kemi* **1969**, *31*, 377−390.
(23) Gans, P.; Sabatini, A.; Vacca, A. *J. Chem. Soc., Dalton Trans.* **1985**, 1195−1200.
(24) Anderegg, G.; L'Eplattenier, F.; Schwarzenbach, G. *Helv. Chim. Acta* **1963**, *46*, 1400−1408.
(25) Hernlem, B. J.; Vane, L. M.; Sayles, G. D. *Inorg. Chim. Acta* **1996**, *244*, 179−184.

Table 1. Protonation Constants of Desferrioxamine B (DFO-B) and Equilibrium Constants of Pu(IV) Complexation with DFO-B at $I = 0.10$ M $NaNO_3$[a]

reaction	thermodynamic parameters	data from the literature
$Fe(III) + H_2O \rightleftharpoons Fe(OH)^{2+} + H^+$		$\log *\beta_{1,1} = -2.51$[b]
$Fe(III) + 2H_2O \rightleftharpoons Fe(OH)_2^{+} + 2H^+$		$\log *\beta_{2,1} = -5.76$[b]
$2Fe(III) + 2H_2O \rightleftharpoons Fe_2(OH)_2^{4+} + 2H^+$		$\log *\beta_{2,2} = -3.06$[b]
$Pu(IV) + H_2O \rightleftharpoons Pu(OH)^{3+} + H^+$		$\log *\beta_{1,1} = -0.05$[c]
$Pu(IV) + 2H_2O \rightleftharpoons Pu(OH)_2^{2+} + 2H^+$		$\log *\beta_{2,1} = -0.49$[c]
$Pu(IV) + 3H_2O \rightleftharpoons Pu(OH)_2^{+} + 3H^+$		$\log *\beta_{3,1} = -3.61$[c]
$Pu(IV) + 4H_2O \rightleftharpoons Pu(OH)_4 + 4H^+$		$\log *\beta_{4,1} = -9.82$[c]
$H_1DFO\text{-}B^- \rightleftharpoons DFO\text{-}B^{2-} + H^+$	$pKa_1 = 9.71 \pm 0.16$	9.70[d]−9.55[e]
$H_2DFO\text{-}B \rightleftharpoons H_1DFO\text{-}B^- + H^+$	$pKa_2 = 8.97 \pm 0.16$	9.03[d]−8.98[e]
$H_3DFO\text{-}B^+ \rightleftharpoons H_2DFO\text{-}B + H^+$	$pKa_3 = 8.35 \pm 0.10$	8.39[d]−8.32[e]
$Pu(IV) + DFO\text{-}B^{2-} + 2H^+ \rightleftharpoons Pu(IV)H_2(DFO\text{-}B)^{4+}$	$\log \beta_{1,1,2} = 35.48 \pm 0.50$	
$Pu(IV) + DFO\text{-}B^{2-} + H^+ \rightleftharpoons Pu(IV)H(DFO\text{-}B)^{3+}$	$\log \beta_{1,1,1} = 34.87 \pm 0.30$	
$Pu(IV) + DFO\text{-}B^{2-} \rightleftharpoons Pu(IV)(DFO\text{-}B)^{2+}$	$\log \beta_{1,1,0} = 33.98 \pm 0.90$[g]	30.8[f]
	$\log \beta^{\circ}_{1,1,0} = 35.76 \pm 0.90$[h]	
$Pu(IV) + DFO\text{-}B^{2-} + H_2O \rightleftharpoons Pu(IV)(DFO\text{-}B)(OH)^{+}$	$\log K_{1,1,-1} = 27.33 \pm 0.05$[i]	
$Pu(IV) + 2DFO\text{-}B^{2-} + 2H^+ \rightleftharpoons Pu(IV)H_2(DFO\text{-}B)_2^{2+}$	$\log \beta_{2,1,2} = 62.30 \pm 0.19$[j]	

[a] The overall stability constants of the complex $M_mL_lH_h$ are expressed as $\beta_{l,m,h}$. [b] Data from ref 9. [c] Data from ref 10. [d] Data from ref 24 at $I = 0.10$ M $NaNO_3$. [e] Data from ref 25 at $I = 0.10$ M KNO_3. [f] From ref 32. [g] Determined from EDTA competition experiments. [h] Extrapolated to zero ionic strength using the SIT theory. [i] Determined from spectrophotometric titrations. [j] Determined from potentiometric titrations.

in strong acid[26] (pH < 0) making it difficult to determine the equilibrium constant for the formation of the complex $Pu(IV)(DFO\text{-}B)^{2+}$. Indirect determination of the stability constant by measuring the fraction of Pu(IV) bound to DFO-B relative to EDTA was used. Competition experiments were carried out by mixing solutions containing Pu(IV), DFO-B, and EDTA in the p[H$^+$] range from 0.50 to 1.0, and 0.10 M $NaNO_3$. The absorbance spectra of the solutions were measured immediately after mixing all the reagents. The absorption intensities of the solutions containing EDTA were lower than controls set at the same conditions without EDTA. The spectra of solutions containing EDTA (at p[H$^+$] 2.0) did not change to any significant degree after a prolonged equilibration time (24 h), indicating that the equilibrium is rapidly established after mixing the reagents. The rapid establishment of equilibrium is in agreement with the fast ligand-exchange properties of Pu(IV), as exemplified by the rate of water exchange for $Pu(IV)(H_2O)_9^{4+}$ $k_{ex} > 3.16 \times 10^7$ s^{-1}.[27] The equilibrium reaction between EDTA and DFO-B complexes can be described according to eq 2.

$$Pu(IV)(DFO\text{-}B)^{2+} + EDTA^{4-} \rightleftharpoons Pu(IV)(EDTA) + DFO\text{-}B^{2-} \quad (2)$$

The overall stability constant for the formation of the complex $Pu(IV)(DFO\text{-}B)^{2+}$ was determined from eq 3.

$$\beta^{Pu(IV)(DFO-B)}_{1,1,0} = \frac{\beta^{Pu(IV)(EDTA)}_{1,1,0}\alpha_{Pu(IV)(EDTA)}\alpha_{DFO-B}9X}{\alpha_{EDTA}\alpha_{Pu(IV)(DFO-B)}(1-X)} \quad (3)$$

Where α is the Ringbom coefficient,[28] X the fraction of the Pu(IV)(EDTA) complex formed, $\beta_{l,m,h}$ is the overall formation constant of the complex $M_mL_lH_h$.

The determination of the equilibrium constant for Pu(IV) binding to natural siderophores by competition with EDTA is a good alternative to direct measurements. However; since Pu(IV) can accommodate more than six donor groups in its first coordination shell, ternary complexes Pu(IV)(siderophore)$_2$, Pu(IV)(EDTA)$_2$, and Pu(IV)(siderophore)(EDTA) can form. It is therefore important to perform the competition experiments in the pH domain where only Pu(IV)(siderophore) and Pu(IV)(EDTA) are formed. Effectively, careful p[H$^+$] control minimizes the formation of ternary complexes. The EDTA complexes formed with Pu(IV) are fairly well characterized.[17] Under the p[H$^+$] conditions examined here (p[H$^+$] from 0.50 to 1.0), the main aqueous complexes formed are $Pu(IV)H_2(DFO\text{-}B)^{4+}$, $Pu(IV)H_1(DFO\text{-}B)^{3+}$, $Pu(IV)(DFO\text{-}B)^{2+}$, and Pu(IV)(EDTA). The decrease in the absorbances of the Pu(IV)(DFO-B) solutions containing EDTA relative to the control solutions without added EDTA at the same p[H$^+$] were used to determine the fraction of Pu(IV) complexed by EDTA. The fraction of Pu(IV) bound to EDTA at p[H$^+$] from 0.50 to 1.0 did not vary significantly. The average of four measurements at p[H$^+$] from 0.50 to 1.0 were used to determine the overall stability constant of the complex $Pu(IV)(DFO\text{-}B)^{2+}$. The overall stability constant for the complex Pu(IV)(EDTA) in 0.10 M $NaNO_3$ was fixed at $\log \beta_{1,1,0} = 29.04$. This value was extrapolated from our previous data in 1.0 M sodium perchlorate[17] using the specific ion interaction theory (SIT) (see details in Supporting Information).[10] The complex hydrolysis constants for Pu(IV)(EDTA) $\log K_{1,1,-1} = -4.35$ and $\log K_{1,1,-2} = -6.73$[17] were also used in the calculation of the Ringbom coefficient $\alpha_{Pu(IV)(EDTA)}$ for Pu(IV)(EDTA) (see eq 3). The formation of the protonated species $Pu(IV)H_2(DFO\text{-}B)^{4+}$ and $Pu(IV)H_1(DFO\text{-}B)^{3+}$ determined by spectrophotometric titrations (presented in the next section) was also taken into consideration for the calculations of $\alpha_{Pu(IV)(DFO-B)}$. The value

(26) Ghosh, K. K.; Patle, S. K.; Sharma, P.; Rajput, S. K. *Bull. Chem. Soc. Jpn.* **2003**, *76*, 283−290.
(27) Farkas, I.; Grenthe, I.; Banyai, I. *J. Phys. Chem. A* **2000**, *104*, 1201−1206.
(28) Ringbom, A.; Still, E. *Anal. Chim. Acta* **1972**, *59*, 143−146.

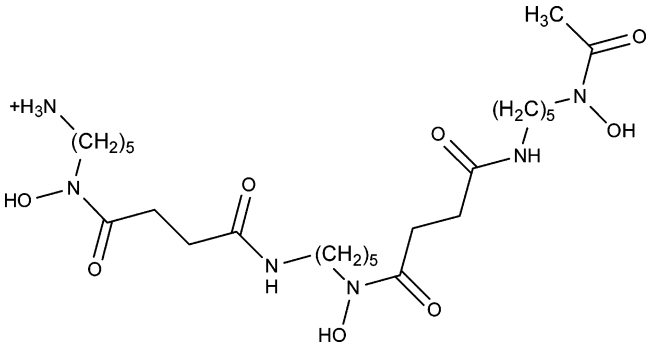

Figure 1. Molecular structure of the natural siderophore desferrioxamine B (DFO-B).

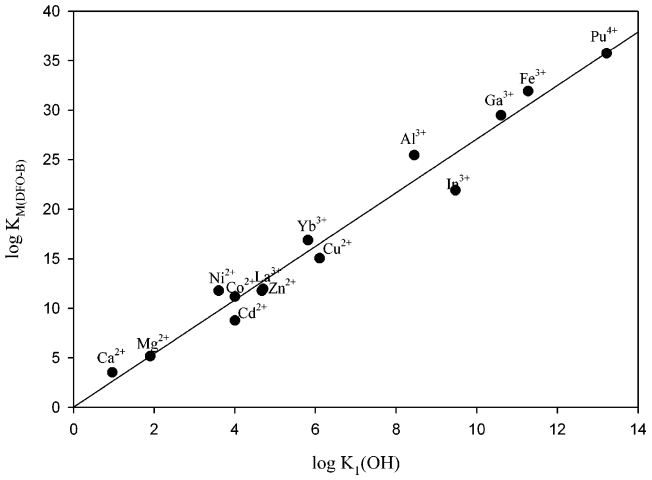

Figure 2. Plot of the overall stability constants of metal binding to DFO-B log $\beta^{\circ}_{1,1,0}$ extrapolated at zero ionic strength as a function of the metal hydrolysis constant. DFO-B metal binding data are from refs 24, 25, and 34, and metal hydrolysis constants are from refs 9 and 10.

of the overall stability constant for the complex $Pu(IV)(DFO\text{-}B)^{2+}$ was determined to be log $\beta_{1,1,0} = 33.98 \pm 1.00$.

The value of the stability constant determined here for the formation of the $Pu(IV)(DFO\text{-}B)^{2+}$ complex in 0.10 M $NaNO_3$, along with the stability constants for other metals from the literature, were extrapolated to zero ionic strength using SIT theory.[10] The calculations were simplified by assuming that the coefficient of specific ion interactions does not significantly affect the activity coefficients of DFO-B and its metal complexes at low ionic strength. The overall stability constant for the formation of $Pu(IV)(DFO\text{-}B)^{2+}$ at zero ionic strength was estimated to be log $\beta^{\circ}_{1,1,0} = 35.76$. The plot of the stability constants for the formation of metal−(DFO-B) complexes at zero ionic strength as a function of the metals hydrolysis constant K_1(OH) is shown in Figure 2. The plot in Figure 2 shows that the value of the overall stability constant for the complex $Pu(IV)(DFO\text{-}B)^{2+}$ determined from the competition experiments is in excellent agreement with the value extrapolated from the plot. The stability constant for Pu(IV) binding is the highest determined for DFO-B. This high binding affinity agrees with the higher Lewis acidity of Pu(IV). The thermodynamic stability constant for Pu(III) binding by DFO-B estimated from the plot in Figure 2 and corrected to 0.10 ionic strength in $NaNO_3$ is log $\beta_{1,1,0} = 17.92$.

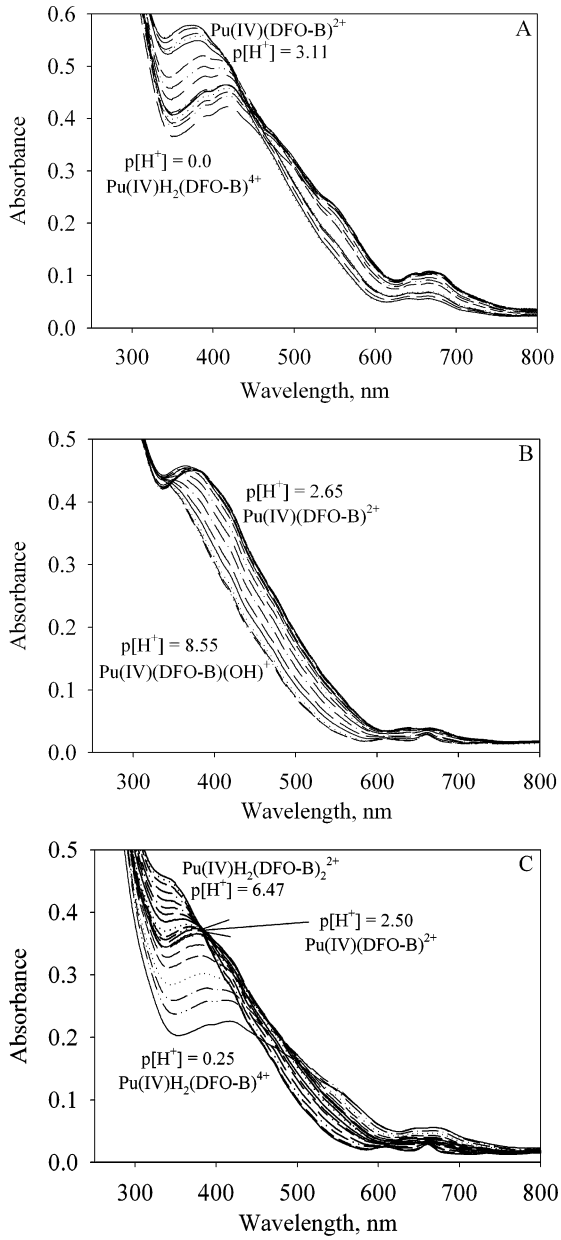

Figure 3. Spectrophotometric titration of $Pu(IV)(DFO-B)^{2+}$ as a function of $p[H^+]$ and Pu(IV)/DFO-B ratio. (A) [Pu(IV)] = [DFO-B] = 0.80 mM, the $p[H^+]$ was varied from 0.0 to 3.11. (B) [Pu(IV)] = [DFO-B] = 0.59 mM, the $p[H^+]$ was varied from 2.65 to 8.55. (C) [Pu(IV)] = 0.59 mM, [DFO-B] = 1.20 mM, the $p[H^+]$ was varied from 0.25 to 6.47. The ionic strength was set at 0.10 M using $NaNO_3$ and the temperature to 25 °C.

Spectrophotometric Characterization of Pu(IV)(DFO-B) Complexes. The spectrophotometric titrations of solutions containing 1:1 and 1:2 Pu(IV)/DFO-B ratios as a function of $p[H^+]$ are shown in Figure 3A−C. The spectral changes observed in strong acid (from $p[H^+]$ 0 to 2.5) for solutions containing 1:1 Pu(IV)/DFO-B and 1:2 Pu(IV)/DFO-B ratios did not vary significantly, which indicates that the complexes formed in acidic solution ($p[H^+] < 2.5$) are not significantly influenced by the Pu(IV)/DFO-B ratio (Figure 3A and C). The UV−visible spectrum of an acidic solution with 1:1 Pu(IV)/DFO-B ($p[H^+] = 0.0$) shows a broad band at 415 nm, a shoulder at 394 nm, and two weak broad bands in the visible region (620−700 nm) (Figure 3A). At higher $p[H^+]$,

the absorbance band at 394 nm shifts to 375 nm and the absorbance band at 415 nm becomes a shoulder (Figure 3A). No isosbestic points were observed in this p[H^+] range, indicating that there are more than two species in equilibrium in solution. These spectral variations are attributed to the successive deprotonations of the complex Pu(IV)H_2(DFO-B)$^{4+}$. The equilibrium reactions involved are described in eqs 4 and 5.

$$\text{Pu(IV)H}_2\text{(DFO-B)}^{4+} \rightleftharpoons \text{Pu(IV)H}_1\text{(DFO-B)}^{3+} + \text{H}^+ \quad (4)$$

$$\text{Pu(IV)H}_1\text{(DFO-B)}^{3+} \rightleftharpoons \text{Pu(IV)(DFO-B)}^{2+} + \text{H}^+ \quad (5)$$

The spectral data recorded in the p[H^+] range between 0.0 and 2.56 were analyzed numerically for the formation of the complexes Pu(IV)H_1(DFO-B)$^{3+}$ and Pu(IV)(DFO-B)$^{2+}$ according to the equilibrium reaction eqs 4 and 5. The overall binding constants for the formation of the species Pu(IV)H_2(DFO-B)$^{4+}$ and Pu(IV)H_1(DFO-B)$^{3+}$ were determined to be log $\beta_{1,1,1} = 34.87 \pm 0.30$ and log $\beta_{1,1,2} = 35.48 \pm 0.50$, respectively. The first protonation constant of the complex Pu(IV)(DFO-B)$^{2+}$, log $K_{\text{Pu(IV)H(DFO-B)}} = 0.89$, agrees with similar values determined for the protonation of the complexes Th(DFO-B)$^{2+}$, Ga(DFO-B)$^{+}$, and Fe(DFO-B)$^{+}$ measured at 1.9,[29] 1.1,[30] and 0.94,[31] respectively. This protonation is assigned to the protonation of the basic N−O oxygen atoms of the hydroxamate groups. This attribution is consistent with the assignment determined from the mechanism of the acid dissociation of the complex Fe(III)(DFO-B) determined though kinetic studies.[21] The value of the protonation of the complexes M(DFO-B) decreases exponentially with the increase of the Lewis acidity of the metal, as shown by the plot in figure S2 (in Supporting Information) showing the decrease of the protonation constant of the complex with the increase of the hydrolysis constant of the metal.

The spectral changes observed above p[H^+] = 2.50 were strongly dependent on the Pu(IV)/DFO-B ratio. The UV−visible spectra of solutions with 1:1 Pu(IV)/DFO-B ratio recorded from p[H^+] 2.56 to 8.55 show a progressive decrease of the absorbance at all wavelengths (Figure 3B). The absorbance maximum at 375 nm gradually shifts to lower wavelength and becomes less defined. No clear isosbestic points were observed. Analysis of the data using a least-squares refinement program LETAGROP-SPEFO[22] with a reaction model that considers the hydrolysis of the complex Pu(IV)(DFO-B)$^{2+}$ (eq 6) yields the value of log $K_{\text{Pu(DFO-B)(OH)}} = -6.65 \pm 0.25$. The spectral changes observed when the solution with 1:2 Pu(IV)/DFO-B ratio was titrated from p[H^+] 0.25 to 6.46 show a progressive shift of the absorbance band at 375 nm to lower wavelengths and an increase in its intensity. A well-defined isosbestic point is observed at 380 nm (Figure 3C). This behavior is distinctive from that observed in the presence of equimolar concentrations of Pu(IV) and DFO-B and is attributed to the formation of a ternary complex Pu(IV)H_2(DFO-B)$_2^{2+}$ according to the equilibrium reaction in eq 7.

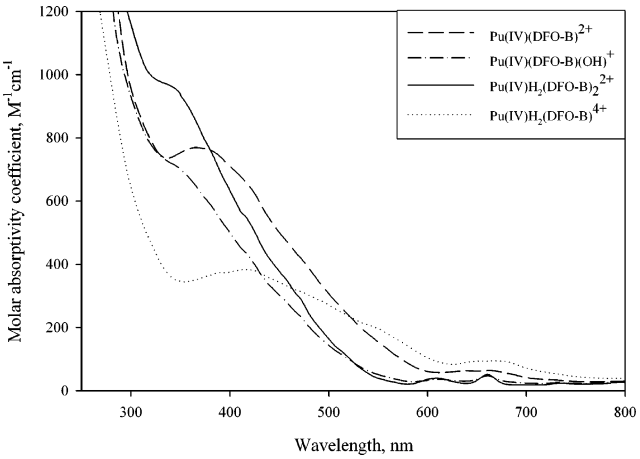

Figure 4. Calculated electronic absorption spectra of the different Pu(IV)(DFO-B) complexes. The spectra were calculated from the Pu(IV)-(DFO-B) experimental spectra using the thermodynamic parameters in Table 1.

$$\text{Pu(IV)(DFO-B)}^{2+} + \text{H}_2\text{O} \xrightleftharpoons{K_{\text{Pu(IV)(DFO-B)OH}}} \text{Pu(IV)(DFO-B)(OH)}^{+} + \text{H}^+ \quad (6)$$

$$\text{Pu(IV)(DFO-B)}^{2+} + \text{H}_3\text{DFO-B}^{+} \xrightleftharpoons{K_{\text{Pu(IV)H2(DFO-B)}_2}} \text{Pu(IV)H}_2\text{(DFO-B)}_2^{2+} + \text{H}^+ \quad (7)$$

The refinement of the spectrophotometric data for the formation of the Pu(IV)H_2(DFO-B)$_2^{2+}$ complex best fit the experimental data. The value of the stability constant for the formation of the complex Pu(IV)H_2(DFO-B)$_2^{2+}$ was determined to be log $\beta_{2,1,2} = 62.30 \pm 0.19$. Table 1 lists the values of the thermodynamic parameters determined in this study along with the values from other studies included for comparison. The calculated electronic absorbance spectra of the different species formed in solution are shown in Figure 4.

Comparative Fe(III)- and Pu(IV)(DFO-B) Binding. Desferrioxamine B is a hexadentate ligand and a single molecule can fully satisfy Fe(III) coordination. The speciation diagram for the Fe(III)(DFO-B) system is dominated by the species Fe(III)(DFO-B)$^{+}$ in the entire pH domain. The speciation diagram for the Pu(IV)(DFO-B) system is significantly different (Figure S3A and B in Supporting Information). The main species formed at neutral pH in equimolar concentration of Pu(IV) and DFO-B is Pu(IV)-(DFO-B)(OH)$^{+}$. At higher pH, Pu(IV) can accommodate multiple hydroxides and in excess DFO-B, Pu(IV) can even accommodate binding groups from a second DFO-B molecule. These results show the fundamental differences

(29) Whisenhunt, D. W.; Neu, M. P.; Hou, Z. G.; Xu, J.; Hoffman, D. C.; Raymond, K. N. *Inorg. Chem.* **1996**, *35*, 4128−4136.
(30) Borgias, B. A.; Barclay, S. J.; Raymond, K. N. *J. Coord. Chem.* **1986**, *15*, 109−123.
(31) Schwarzenbach, G.; Schwarzenbach, K., *Helv. Chim. Acta* **1963**, *46*, 1390−1400.
(32) Jarvis, N. V.; Hancock, R. D. *Inorg. Chim. Acta* **1991**, *182*, 229−232.
(33) Spasojevic, I.; Armstrong, S. K.; Brickman, T. J.; Crumbliss, A. L. *Inorg. Chem.* **1999**, *38*, 449−454.
(34) Evers, A.; Hancock, R. D.; Martell, A. E.; Motekaitis, R. J. *Inorg. Chem.* **1989**, *28*, 2189−2195.

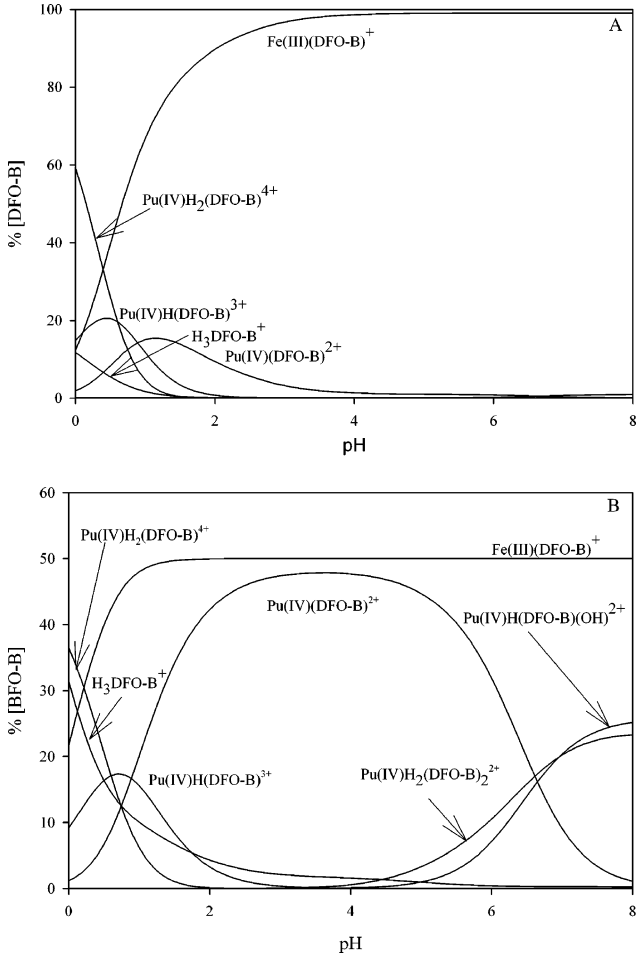

Figure 5. Speciation diagrams showing the competition between Pu(IV) and Fe(III) for DFO-B binding. Conditions: thermodynamic parameters for Pu(IV) and Fe(III) binding from Table 1, (A) [Fe(III)] = [Pu(IV)]= [DFO-B] = 1.0×10^{-6} M, (B) [DFO-B] = 2.0×10^{-6} M, [Fe(III)] = [Pu(IV)] = 1.0×10^{-6} M. Pu(IV) and Fe(III) metal hydrolysis equilibria are included.

between Fe(III) and Pu(IV) coordination properties and the effect of ligand availability on Pu speciation. The concentration of Fe(III) in the media is an important parameter that affects Pu(IV)siderophore speciation. Figure 5A and B shows the species distribution for the ternary system Fe(III), Pu(IV), and DFO-B. Under equimolar concentrations of Fe(III), Pu(IV), and DFO-B, the speciation diagram is dominated by the iron complex $Fe(III)(DFO\text{-}B)^{+}$ above pH 4. At lower pH, both Pu(IV)- and Fe(III)(DFO-B) complexes are present, with $Fe(III)(DFO\text{-}B)^{+}$ being the main complex formed (Figure 5A). Although the overall formation constant for the complex $Pu(IV)(DFO\text{-}B)^{2+}$ $\log \beta_{1,1,0} = 33.98$ is significantly higher than that of $Fe(III)(DFO\text{-}B)^{+}$ $\log \beta = 30.6$,[24] Fe(III) complexes predominate. This is because Pu(IV) is a much stronger Lewis acid compared to Fe(III) and its affinity for the hydroxyl anion (OH^{-}) is much stronger, as can be deduced by comparing Pu(IV) and Fe(III) hydrolysis (Table 1). The high affinity of Pu(IV) for the hydroxyl ion reduces its effective binding to DFO-B relative to that of Fe(III). The speciation diagram in Figure 5B calculated for the ternary system Fe(III), Pu(IV), and DFO-B in the presence of 2 equiv of DFO-B

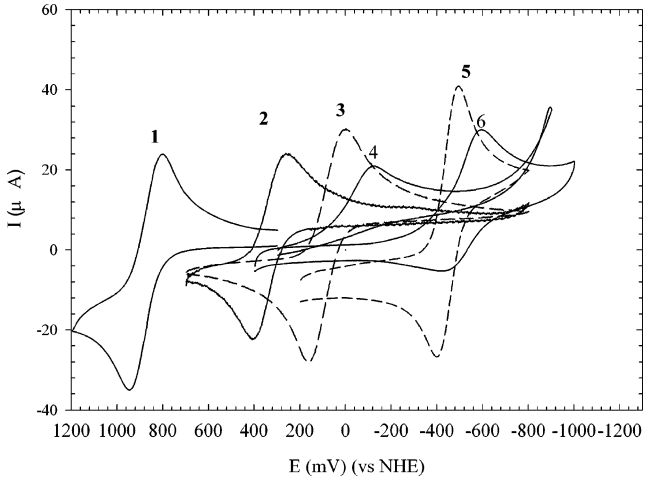

Figure 6. Cyclic voltammograms of selected Pu(IV) and Fe(III) complexes. Conditions: (1) Pu(IV/III)aq in 1.0 M $HClO_4$, [Pu(IV)] = 2.0 mM, I = 1.0 M $NaNO_3$ (2) Pu(IV/III)(EDTA) at pH 2.56, [Pu(IV)(EDTA)] = 2.0 mM, I = 0.10 M $NaNO_3$ (3) Fe(III/II)(EDTA) at pH 2.00, [Fe(III)-(EDTA)] = 2.0 mM, I = 0.10 M $NaNO_3$ (4) Pu(IV/III)(DFO−B) at pH 2.50, I = 0.10 M $NaNO_3$ (5) Fe(III/II) (DFO−B) at pH 4.0, [Fe(III)(DFO−B)] = 2.0 mM (6) $Pu(IV)(DFO\text{-}B)_2$ at pH 6.71, [Pu(IV)(DFO-B)] = 2.0 mM. The cyclic voltammograms were recorded using a standard three electrode cell, T = 25 °C, I = 0.10 M $NaNO_3$ and a scan rate of 100 mV/s.

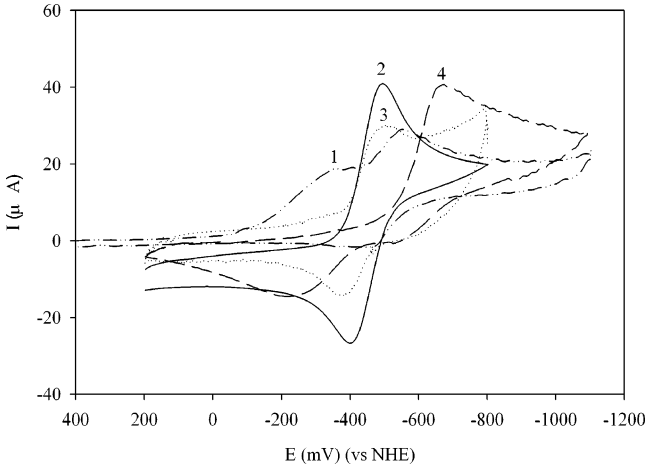

Figure 7. Cyclic voltammograms of $Pu(IV)(siderophore)_2$ complexes obtained using large excess of siderophore over Pu(IV). (1) Pu(IV)-$(rhodotorulic\ acid)_2$ at pH = 8.43 [Pu(IV)] = 2.0 mM, [rhodotorulic acid] = 50 mM, I = 0.10 M $NaNO_3$, (2) Fe(III/II) (DFO-B) at pH 4.0, [Fe(III)-(DFO-B)] = 2.0 mM, (3) $Pu(IV)(pyoverdin)_2$ at pH = 9.41 [Pu(IV)] = 2.0 mM, [pyoverdin] = 50 mM, I = 0.10 M $NaNO_3$, (4) $Pu(IV)(DFO\text{-}E)_2$ at pH = 6.95 [Pu(IV)] = 2.0 mM, [DFO-E] = 50 mM, I = 0.10 M $NaNO_3$. The cyclic voltammograms were recorded using a standard three-electrode cell, T = 25 °C, I = 0.10 $NaNO_3$ and a scan rate of 100 mV/s.

and 1 equiv of Fe(III) and Pu(IV) indicate Pu(IV)-$(DFO\text{-}B)^{2+}$ and $Fe(III)(DFO\text{-}B)^{2+}$ coexist when sufficient DFO-B is present. This result illustrates the strong effect of Fe(III) and DFO-B concentrations on Pu(IV)(DFO-B) speciation.

Electrochemical Behavior of Pu(IV)(siderophore) Complexes. Most siderophores are likely to form stable and soluble complexes with Pu(IV) and therefore affect the interactions of Pu(IV) with microorganisms and the mobility of Pu(IV) in contaminated soils. The high stability and solubility of Pu(IV)siderophore complexes might enhance plutonium mobility in the environment. However, under anoxic and slightly reducing conditions, the reduction of Pu-

Table 2. Redox Potentials of Pu(IV) and Fe(III) Complexes at Identical Conditions.

plutonium complexes	$E_{1/2}$ in V vs NHE	$\log(\beta_{Pu(IV)}/\beta_{Pu(III)})$	iron complexes	$E_{1/2}$ in V vs NHE
$Pu(IV)(H_2O)_9^{4+}$	+0.953		$Fe(III)(H_2O)_6$	+0.77
Pu(IV)(EDTA)	+0.342	10.35	$Fe(III)(EDTA)^-$	+0.134
	+0.320[a]			
$Pu(IV)(DFO\text{-}B)^{2+}$	−0.265[a]	20.6	$Fe(III)(DFO\text{-}B)^+$	−0.448
$Pu(IV)H_2(DFO\text{-}B)_2^{2+}$	−0.509			
$Pu(IV)(DFO\text{-}E)^+$	−0.264[a]	20.6	Fe(III)(DFO-E)	−0.447
$Pu(IV)H_2(DFO\text{-}E)_2$	−0.550			
Pu(IV)(rhodotorulic acid)	−0.239[a]	20.2	Fe(III)(rhodotorulic acid)	−0.422[b]
Pu(IV)(rhodotorulic acid)$_2$	−0.455	−		
Pu(IV)(pyoverdin)	−0.297[a]	21.2	Fe(III)(pyoverdin)	−0.480[c]
Pu(IV)(pyoverdin)$_2$	−0.440			

[a] Estimated by assuming that the difference between Pu(IV/III)aq and Fe(III/II)aq couple which is conserved in Pu(IV/III)(EDTA) and Fe(III/II)(EDTA) is also conserved in the complexes Pu(IV/III)(siderophores), Fe(III/II)(siderophores). [b] From ref 33. [c] From ref 18.

(IV)(siderophore) complexes may considerably reduce the stability of the complexes formed. The increase of soluble iron under reducing conditions can also affect the formation of Pu(IV)(siderophore) complexes. The examination of the redox behavior of Pu(IV) complexes with a number of natural siderophores was carried out to determine the redox behavior of Pu(IV)(siderophore) complexes and their consequences on plutonium mobility in the environment.

The redox behavior of Pu(IV) complexes formed with the natural siderophores desferrioxamine B, desferrioxamine E, pyoverdin, and rhodotorulic acid was examined by cyclic voltammetry. The redox behavior of their analogous ferric complexes was also determined for comparison. The redox potentials of Fe(III/II) complexes are usually lower than the redox potentials of Pu(IV/III) complexes when bound to the same ligand. The shift between the redox potential of Fe(III) complexes and the redox potentials of their Pu(IV) analogues is about the same as the difference between the redox potential of their fully hydrated ions ($E°_{aq}$ for $Fe(III)(H_2O)_6^{3+}$ is 0.77 V and is about 0.18 V lower than $E°_{aq}$ for $Pu(IV)(H_2O)_9^{4+}$ = + 0.95 V). The redox potential of $Fe(III)(EDTA)^-$ ($E_{1/2}$ = + 0.134 V) determined from the cyclic voltammogram of the complex shown in Figure 6 curve 3, is about 0.20 V lower than that of Pu(IV)(EDTA) ($E_{1/2}$ = + 0.342 V) shown in Figure 6, curve 2. The redox potential of Pu(IV)- and Fe(III)(siderophore) complexes examined were all lower than the redox potential of their fully hydrated cations, which indicates that siderophores have lower affinities for Fe(II) and Pu(III). The cyclic voltammograms of $Pu(IV)(DFO\text{-}B)^{2+}$ complexes formed with 1:1 Pu(IV)/DFO-B at different pHs are irreversible. The cyclic voltammograms show a reduction wave at about −0.05 V without its reoxidation counter part (Figure 6, curve 4). This behavior is attributed to the fast acid dissociation of the unstable $Pu(III)(DFO\text{-}B)^+$ complex. However, in excess DFO-B over Pu(IV), the cyclic voltammogram recorded at pH 6.71 shows quasi-reversible behavior (Figure 6, curve 6). The redox potential determined $E_{1/2}$ = −0.509 V is slightly more negative than that of $Fe(III)(DFO{-}B)^+$ $E_{1/2}$ = −0.480 V (Figure 6, curve 5). Quasi-reversible behavior was obtained only when using large excesses of siderophores over Pu(IV) and near neutral pH. Under these conditions the complexes formed have a 1:2 Pu(IV)/siderophore stoichiometry. The cyclic voltammogram of Pu(IV)(pyoverdin)$_2$ (Figure 7) recorded at pH 9.41 shows a quasi-reversible wave with 137 mV peak to peak separation. The redox potential of the electrochemical process recorded was determined to be $E_{1/2}$ = −0.440 V. The redox potentials determined from solutions containing excess desferrioxamine E and rhodotorulic acid over Pu(IV) are $E_{1/2}$ = −0.550 and −0.455 V, respectively.

Comparing the redox potentials of Fe(III)(siderophore) and Pu(IV)(siderophore) complexes is complicated by the fact that plutonium can accommodate more binding groups in its first coordination shell than iron. At neutral pH, Fe(III) is fully complexed (coordinatively saturated) by one siderophore molecule. However, $Pu(IV)(DFO\text{-}B)^{2+}$ can accommodate multiple hydroxides and even a second DFO-B molecule. In their coordinatively saturated form, Pu(IV) complexes can accommodate up to 12 oxygen donor groups, making the Pu(IV) environment more electron rich and therefore harder to reduce. Consequently, it is not surprising to observe redox potentials for Pu(IV)(siderophore)$_2$ complexes that are more negative than the Fe(III)(siderophore) complexes. The redox potentials of the 1:1 Pu(IV)/siderophore could not be determined. Reversible voltammograms for the 1:1 Pu(IV)/siderophore complexes could not be obtained because of the low stability of Pu(III)(siderophore) complexes in acid and the hydrolysis of Pu(IV)(siderophore) complexes at higher pH. The addition of excess siderophore results in the formation of 1:2 Pu(IV)/siderophore complexes.

The redox potentials of 1:1 Pu(IV)/siderophore complexes were estimated from the redox potentials of Fe(III)(siderophore) by assuming that the shift in the redox potential of the aquated Fe(III/II) couple upon siderophore binding is equivalent to the shift in the Pu(IV/III) couple upon binding to the same siderophore. When applied to the redox potentials of $Fe(III)(EDTA)^-$ and Pu(IV)(EDTA), the estimated Pu(IV)(EDTA) redox potential is $E_{1/2}$ = 0.320 V. This redox potential is close to the value of the redox potential for the complex Pu(IV)(EDTA) determined experimentally $E_{1/2}$ = + 0.342 V. The redox potentials of the 1:1 Pu(IV)/siderophore complexes estimated are situated at 0.20 V higher than their Fe(III)(siderophore) analogues (Table 2). These estimated redox potentials were used to determine the upper limits for the differences between siderophore binding for Pu(IV) and Pu(III). The data in Table 2 indicate that Pu(III)(siderophore) complexes are more than 20 orders of

magnitude less stable than their Pu(IV) analogues. This indicates that under anoxic and environmentally reducing conditions, the stability of Pu(siderophore) complexes is significantly reduced.

Summary and Conclusions

Siderophore complexes of Pu(IV) are soluble and very stable. The characterization of Pu(IV) coordination, stability, and redox behavior with these natural ligands is important in order to understand their possible impact on the stability and bioavailability of Pu species in the environment. Siderophores, which are common organic chelators present in soils, can form different soluble complexes with different stoichiometries depending on the pH and ligand availability. The determination of the thermodynamic properties of Pu(IV) complexes formed with natural ligands and siderophores in particular is very difficult. The determination of the stability constants of complexes formed in acid is complicated by the fact that natural siderophores are not very stable in acid. Under conditions sufficiently acidic to have equilibrium between free and complexed Pu, the siderophore hydrolyzes very rapidly. However, at higher pH where natural siderophores are stable, the complexes are already formed and the thermodynamic parameters cannot be determined. The use of competition reactions with well characterized ligands such as EDTA can be effective for the determination of the binding constants for Pu(IV)(siderophores). However, the accuracy of the values determined is dependent on the accuracy of the parameters used for the competing ligand. The formation of ternary complexes Pu(IV)(siderophore)(EDTA) is a major limitation for this method.

Competition experiments were successfully used to determine the binding constant for the complex Pu(IV)(DFO-B)$^{2+}$ through the utilization of EDTA. The competition reactions were set at p[H$^+$] ranging from 0.5 to 1.0 where the formation of the ternary complexes could be neglected and where DFO-B was sufficiently stable. The value of the stability constant determined ($\log \beta_{1,1,0} = 33.98$) is the highest measured for DFO-B with any metal. This value is supported by the high Lewis acidity of Pu(IV) which favors its binding to ligands with hard oxygen donor groups. Since one DFO-B molecule cannot provide full Pu(IV) coordination, at higher pH, hydrolysis products Pu(IV)(DFO-B)$(OH)_x(H_2O)_n$ and also ternary complexes Pu(IV)(DFO-B)$_2(H_2O)_n$ are formed. The thermodynamic properties of the complex Pu(IV)(DFO-B)(OH)$^+$ was determined to be $\log K = -6.65$, and the formation constant for the complex Pu(IV)H$_2$(DFO-B)$_2^{2+}$ was determined to be $\log K = 62.30$.

The examination of the redox properties of Pu(IV)(DFO-B) complex by cyclic voltammetry indicates that DFO-B does not bind Pu(III) very well. The DFO-B binding constant was estimated to be more than 20 orders of magnitude lower than that of Pu(IV). This behavior was consistent among other natural siderophores examined. The Pu(III) complexes of pyoverdin, desferrioxamine E and rhodotorulic acid were all found to be unstable. The redox potential of the 1:1 Pu(IV)/siderophore complexes were estimated to be about 0.20 V higher than their Fe(III)-(siderophore) analogues. The redox potentials of Pu(IV)-(siderophores)$_2$ complexes determined by cyclic voltammetry were found to be slightly lower than the redox potentials of the 1:1 Fe(III)/siderophore complexes.

Acknowledgment. We thank the Environmental Remediation Sciences Division Research program (ERSD), Office of Biological and Environmental Research, Office of Science, of the U.S. Department of Energy for financial support.

Supporting Information Available: Figure S1 showing the potentiometric titrations of free DFO-B and its Pu(IV) complexes, Figure S2 showing the plot of log $K_{MH(DFO-B)}$ as a function of the metal hydrolysis constant, Figure S3 showing the speciation diagrams for Pu(IV) complexes with DFO-B and the details of the extrapolation of the stability constants of the complexes Pu(IV)-(EDTA) and Pu(IV)(DFO-B)$^{2+}$ to zero ionic strength using the SIT theory. This material is available free of charge via the Internet at http://pubs.acs.org.

IC061544Q